Experimental design to measure the anchoring energy on substrate surface by using the alternating-current bridge*

Hui-Ming Hao(郝慧明)[1], Yao-Yao Liu(刘瑶瑶)[1], Ping Zhang(张平)[1], Ming-Lei Cai(蔡明雷)[2,3], Xiao-Yan Wang(王晓燕)[2,3], Ji-Liang Zhu(朱吉亮)[1], and Wen-Jiang Ye(叶文江)[1,†]

[1] *School of Sciences, Hebei University of Technology, Tianjin* 300401, *China*
[2] *Hebei Jiya Electronics Co. Ltd., Shijiazhuang* 050071, *China*
[3] *Hebei Provincial Research Center of LCD Engineering Technology, Shijiazhuang* 050071, *China*

(Received 23 March 2017; revised manuscript received 12 May 2017; published online 20 June 2017)

The anchoring property of the substrate surface of liquid crystal cells plays an important role in display and nondisplay fields. This property directly affects the deformation of liquid crystal molecules to change the phase difference through liquid crystal cells. In this paper, a test method based on the alternating-current bridge is proposed to determine the capacitance of liquid crystal cells and thus measure the anchoring energy of the substrate surface. The anchoring energy can be obtained by comparing the capacitance–voltage curves of twisted nematic liquid crystal cells with different anchoring properties in experimental and theoretical results simulated on the basis of Frank elastic theory. Compared with the other methods to determine the anchoring energy, our proposed method requires a simple treatment of liquid crystal cells and allows easy and high-accuracy measurements, thereby expanding the test ideas on the performance parameters of liquid crystal devices.

Keywords: anchoring energy, alternating-current bridge, capacitance of liquid crystal cell, twisted nematic

PACS: 61.30.Dk, 64.70.mj **DOI:** 10.1088/1674-1056/26/8/086102

1. Introduction

Liquid crystal (LC) materials, as a type of transmission medium, are widely used in display and nondisplay fields because of their capacity to modulate the outside signal and the control voltage.[1] The uniform orientation of LC molecules in LC devices significantly influences the result of LC modulation. The alignment layer on the substrate surface determines the uniform orientation of LC molecules, i.e., the anchoring characteristics of the alignment layers to LC molecules.[2] The LC molecule deformation in LC cells with different anchoring strengths is different even when the applied voltage is the same. At present, several LC display and nondisplay devices are based on weak anchoring.[3–9] Therefore, the precise determination of anchoring energy on the substrate surface can ensure the accurate design of LC devices.

Anchoring treatment on the surface can be classified as either contact type or noncontact type. Contact type, that is, rubbing the substrate, is the main treatment currently used in industrial production. Noncontact type, including oblique evaporation[10] and photoinduced alignment,[11] is the major treatment used in laboratory research. To connect with industrial production, the anchoring effect caused by rubbing the substrate should be considered. Anchoring energy can be measured by using optical and electrical methods. The optical method has two main types: Freedericksz transition technology[12,13] and optical waveguide technology.[14] The former requires the electromagnetic coherence length to be approximately the same as the LC cell thickness, indicating that the Freedericksz transition can occur only when the surface has strong anchoring. The latter is a relatively high-precision measurement, but the experiment equipment and data processing are complicated, which can easily cause errors. The main electrical method is the high electric field technique.[15,16] In the real measurement system, however, LCs may contain a small amount of conductive ion and flexelectric effect, which could affect the measurement result. An electrical measurement method to obtain the anchoring energy of the substrate surface is achieved by comparing the experimental *C–U* curve with a numerical simulation *C–U* curve based on Frank elastic theory.[17,18] Ye *et al.*[19] determined the influence of substrate anchoring on the capacitance of parallel alignment nematic and hybrid alignment nematic LC cells through theoretical analysis and numerical simulation. In the present paper, we propose an experimental design to measure the capacitance of twisted nematic (TN) LC cells and thus obtain the anchoring energy on the substrate surface using the alternating-current (AC) bridge.

*Project supported by the National Natural Science Foundation of China (Grant Nos. 11374087 and 11504080), the Natural Science Foundation of Hebei Province, China (Grant Nos. A2014202123 and A2017202004), the Research Project of the Education Department of Hebei Province, China (Grant No. QN2014130), the Key Subject Construction Project of Hebei Provincial University, and the Undergraduate Innovation and Entrepreneurship Training Program, China (Grant No. 201610080016).

†Corresponding author. E-mail: wenjiang_ye@hebut.edu.cn

© 2017 Chinese Physical Society and IOP Publishing Ltd

2. Theoretical basis

In our proposed method, the anchoring energy is measured by comparing the *C–U* curves of experimental results and theoretical simulation. Two basic theories are involved, namely, the capacitance determination of LC cells on the basis of the AC bridge and the numerical simulation of the capacitance of LC cells on the basis of Frank elastic theory.

2.1. AC bridge

The schematic of the AC bridge is shown in Fig. 1, where S is the AC signal source, R_i ($i = x$, 2, 3, 4) is a precision adjustable resistance, C_x is the LC cell to be measured, C_2 is the precision fixed value capacitor, G is the galvanometer, and K is the switch.

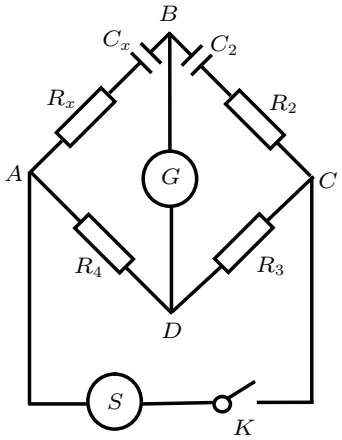


Fig. 1. Schematic diagram of the AC bridge.

When the bridge reaches balance, points B and D have the same voltage amplitude and phase, that is to say, $U_B = U_D$ and $\varphi_B = \varphi_D$, which meet the following relationship:

$$\tilde{U}_B = \tilde{U}_D. \tag{1}$$

From Eq. (1), one can obtain

$$\begin{cases} R_x = \dfrac{R_4}{R_3} R_2, \\ C_x = \dfrac{R_3}{R_4} C_2, \\ \tan\varphi' = \omega C_2 R_2 = \omega C_x R_x, \end{cases} \tag{2}$$

where φ' is the phase difference between B and D, and ω is the angular frequency of AC signal.

2.2. Numerical simulation of capacitance of TN cell

The structure of the weak anchoring TN cell is shown in Fig. 2, with the thickness of l, and the alignment layers on the upper and lower substrates are rubbed in the x and y directions, respectively. The LC molecules are distorted by 90° from the lower to the upper substrate. The anchoring directions of the upper and lower substrates are $\boldsymbol{e}_l$ and $\boldsymbol{e}_0$, respectively, in which the pretilt angles are Θ_l and Θ_0, and the pretwist angles are Φ_l and Φ_0. The LC director $\boldsymbol{n}$ is determined by the tilt angle θ and twist angle ϕ, and is only a function of the spatial coordinate z. The electric field in the cell formed by the applied voltage U changes the orientation of the LC molecules, which can be determined on the basis of Frank elastic theory.

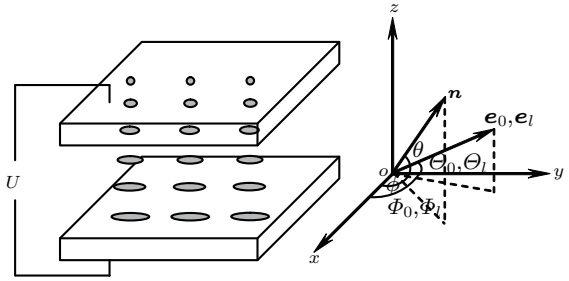


Fig. 2. The structure of a TN cell with a weak anchoring and coordinate system.

The free energy of the TN cell system per unit area is

$$F = \int_0^l f_z \mathrm{d}z + F_{s0} + F_{sl}, \tag{3}$$

where f_z is the free energy density, and F_{s0} and F_{sl} are the surface anchoring energy per unit area of the lower and upper substrates, respectively. Their expressions are

$$\begin{aligned} f_z = {} & \frac{1}{2}\left[f(\theta)\left(\frac{\mathrm{d}\theta}{\mathrm{d}z}\right)^2 + g(\theta)\left(\frac{\mathrm{d}\phi}{\mathrm{d}z}\right)^2\right] - \frac{\varepsilon_0}{2}\left(\frac{\mathrm{d}U}{\mathrm{d}z}\right)^2 h(\theta) \\ & + \frac{1}{2}k_{22}\left(\frac{2\pi}{P}\right)^2 - k_{22}\frac{2\pi}{P}\cos^2\theta\frac{\mathrm{d}\phi}{\mathrm{d}z}, \end{aligned} \tag{4}$$

$$F_{s0} = \frac{1}{2}A_{\theta 0}\sin^2(\theta_0 - \Theta_0) + \frac{1}{2}A_{\phi 0}\sin^2(\phi_0 - \Phi_0), \tag{5}$$

$$F_{sl} = \frac{1}{2}A_{\theta l}\sin^2(\theta_l - \Theta_l) + \frac{1}{2}A_{\phi l}\sin^2(\phi_l - \Phi_l), \tag{6}$$

where $f(\theta) = k_{11}\cos^2\theta + k_{33}\sin^2\theta$, $g(\theta) = (k_{22}\cos^2\theta + k_{33}\sin^2\theta)\cos^2\theta$, k_{11}, k_{22}, and k_{33} are the splay, twist, and bend elastic constants of LC; ε_0 is permittivity in the vacuum; $h(\theta) = \varepsilon_\perp + \Delta\varepsilon\sin^2\theta$, $\Delta\varepsilon = \varepsilon_{||} - \varepsilon_\perp$ are the dielectric anisotropy of LC; $\varepsilon_{||}$ and $\varepsilon_\perp$ are the relative permittivity along the direction parallel and vertical to the molecule long axis of LC, respectively; P is the pitch induced by the chiral dopant; θ_0 and ϕ_0 are the tilt and twist angles of the LC director on the lower substrate; θ_l and ϕ_l are the tilt and twist angles of the LC director on the upper substrate; $A_{\theta 0}$ and $A_{\phi 0}$ are the polar and the azimuthal anchoring energy on the lower substrate; and $A_{\theta l}$ and $A_{\phi l}$ are the polar and the azimuthal anchoring energy on the upper substrate.

When the system reaches balance under an applied voltage, according to the variational principle, the Euler equations including the tilt angle θ, the twist angle ϕ, and the potential ϕ, can be deduced as follows:[20]

$$\frac{\partial f_z}{\partial\theta} - \frac{\mathrm{d}}{\mathrm{d}z}\left[\frac{\partial f_z}{\partial\left(\dfrac{\mathrm{d}\theta}{\mathrm{d}z}\right)}\right] = 0, \tag{7}$$

$$el8\frac{\partial f_z}{\partial \phi} - \frac{\mathrm{d}}{\mathrm{d}z}\left[\frac{\partial f_z}{\partial\left(\frac{\mathrm{d}\phi}{\mathrm{d}z}\right)}\right] = 0, \tag{8}$$

$$\frac{\partial f_z}{\partial \varphi} - \frac{\mathrm{d}}{\mathrm{d}z}\left[\frac{\partial f_z}{\partial\left(\frac{\mathrm{d}\varphi}{\mathrm{d}z}\right)}\right] = 0. \tag{9}$$

Concurrently, the tilt θ and the twist angle ϕ of the LC director on the upper and lower substrates meet the following conditions

$$\left(\frac{\partial f_z}{\partial(\mathrm{d}\theta/\mathrm{d}z)}\right)_l + \frac{\partial F_{sl}}{\partial \theta_l} = 0, \tag{10}$$

$$\left(\frac{\partial f_z}{\partial(\mathrm{d}\phi/\mathrm{d}z)}\right)_l + \frac{\partial F_{sl}}{\partial \phi_l} = 0, \tag{11}$$

$$\left(\frac{\partial f_z}{\partial(\mathrm{d}\theta/\mathrm{d}z)}\right)_0 - \frac{\partial F_{s0}}{\partial \theta_0} = 0, \tag{12}$$

$$\left(\frac{\partial f_z}{\partial(d\phi/dz)}\right)_0 - \frac{\partial F_{s0}}{\partial \phi_0} = 0. \tag{13}$$

Substituting Eqs. (4)–(6) into Eqs. (7)–(13), we can obtain the equilibrium state equations and boundary conditions of the LC cell system

$$f(\theta)\frac{\mathrm{d}^2\theta}{\mathrm{d}z^2} + \sin\theta\cos\theta\left[(k_{33}-k_{11})\left(\frac{\mathrm{d}\theta}{\mathrm{d}z}\right)^2 + \left(2k_{22}\cos^2\theta - k_{33}\cos 2\theta\right)\left(\frac{\mathrm{d}\phi}{\mathrm{d}z}\right)^2 + \Delta\varepsilon\varepsilon_0\left(-\frac{\mathrm{d}U}{\mathrm{d}z}\right)^2 - \frac{4\pi k_{22}}{P}\frac{\mathrm{d}\phi}{\mathrm{d}z}\right] = 0, \tag{14}$$

$$g(\theta)\frac{\mathrm{d}^2\phi}{\mathrm{d}z^2} + 2\sin\theta\cos\theta \times \left[(k_{33}\cos 2\theta - 2k_{22}\cos^2\theta)\frac{\mathrm{d}\phi}{\mathrm{d}z} + \frac{2\pi k_{22}}{P}\right]\frac{\mathrm{d}\theta}{\mathrm{d}z} = 0, \tag{15}$$

$$\frac{\mathrm{d}^2\varphi}{\mathrm{d}z^2}h(\theta) + 2\frac{\mathrm{d}\varphi}{\mathrm{d}z}\Delta\varepsilon\sin\theta\cos\theta\frac{\mathrm{d}\theta}{\mathrm{d}z} = 0, \tag{16}$$

$$f(\theta_l)\left(\frac{\mathrm{d}\theta}{\mathrm{d}z}\right)_l + A_{\theta l}\sin(\theta_l - \Theta_l)\cos(\theta_l - \Theta_l) = 0, \tag{17}$$

$$g(\theta_l)\left(\frac{\mathrm{d}\phi}{\mathrm{d}z}\right)_l - \frac{2\pi k_{22}}{P}\cos^2\theta_l + A_{\phi l}\sin(\phi_l - \Phi_l)\cos(\phi_l - \Phi_l) = 0, \tag{18}$$

$$f(\theta_0)\left(\frac{\mathrm{d}\theta}{\mathrm{d}z}\right)_0 - A_{\theta 0}\sin(\theta_0 - \Theta_0)\cos(\theta_0 - \Theta_0) = 0, \tag{19}$$

$$g(\theta_0)\left(\frac{\mathrm{d}\phi}{\mathrm{d}z}\right)_0 - \frac{2\pi k_{22}}{P}\cos^2\theta_0 - A_{\phi 0}\sin(\phi_0 - \Phi_0)\cos(\phi_0 - \Phi_0) = 0. \tag{20}$$

On the basis of the above equilibrium state equations and the boundary conditions, as well as the differential iteration method in Ref. [21], the distributions of the tilt and twist angles under different applied voltages and anchoring energies can be calculated, as shown in Figs. 3 and 4. In the calculation, LC E7 is considered with the following material parameters:[22] $k_{11} = 10.8$ pN, $k_{22} = 6.8$ pN, $k_{33} = 17.5$ pN, $\varepsilon_{||} = 19.2$, and $\varepsilon_{\perp} = 5.2$. The TN cell thickness is $l = 10$ μm, the pretilt angles on the upper and lower substrates are $\Theta_l = \Theta_0 = 1^\circ$, the pretwist angles are $\Phi_l = 90^\circ$ and $\Phi_0 = 0^\circ$, and the LC pitch is $P \to \infty$. When the applied voltage (2 V) is beyond the threshold, the substrate anchoring energy coefficient significantly influences the tilt angle of the LC director. As the anchoring energy coefficient decreases (from strong to weak anchoring), the LC director near the substrate surface changes substantially, leading to the strong variation of cell capacitance. When the substrate anchoring is weak (10^{-4} J/m^2), the director tilt angle near the substrate surface increases, as the applied voltage is increased, thereby changing the TN cell capacitance.

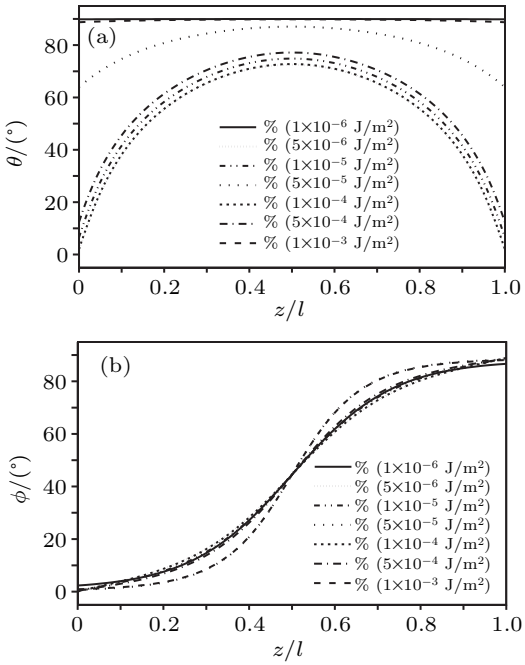


Fig. 3. Director distribution under the applied voltage of 2 V for different anchoring energy coefficients: (a) tilt angle and (b) twist angle.

Once the tilt angle of the LC director at a voltage is determined, the TN cell capacitance can be expressed as[23]

$$C = \frac{S\varepsilon_{\perp}\varepsilon_0}{\int_0^l \frac{\mathrm{d}z}{1+\gamma\sin^2\theta}}, \tag{21}$$

where $\gamma = \Delta\varepsilon/\varepsilon_{\perp}$ and S is the substrate area. To compare conveniently the theoretical and experimental results, the reduced capacitance of the LC cell is introduced, and it can be expressed as

$$c = C/C_0 = 1/\int_0^1 \frac{\mathrm{d}\xi}{1+\gamma\sin^2\theta}, \tag{22}$$

where $\xi = z/l$ and $C_0 = S\varepsilon_{\perp}\varepsilon_0/l$ is the capacitance of the TN cell without voltage application. After the tilt angle of the LC director under different voltages is determined, we can obtain the theoretically reduced capacitance curve of the TN cell

with different substrate anchoring energy coefficients by using Eq. (22) (Fig. 6). The smaller the substrate anchoring energy coefficient (10^{-6} J/m^2), the lower the applied voltage (0.8 V) to make the TN cell capacitance reach a stable value. The steepness of the *C–U* curve decreases as the substrate anchoring energy coefficient is increased. For the two situations of 5×10^{-4} J/m^2 and 10^{-3} J/m^2, the two curves are almost coincident, indicating that the substrate anchoring energy coefficient 5×10^{-4} J/m^2 has reached strong anchoring.

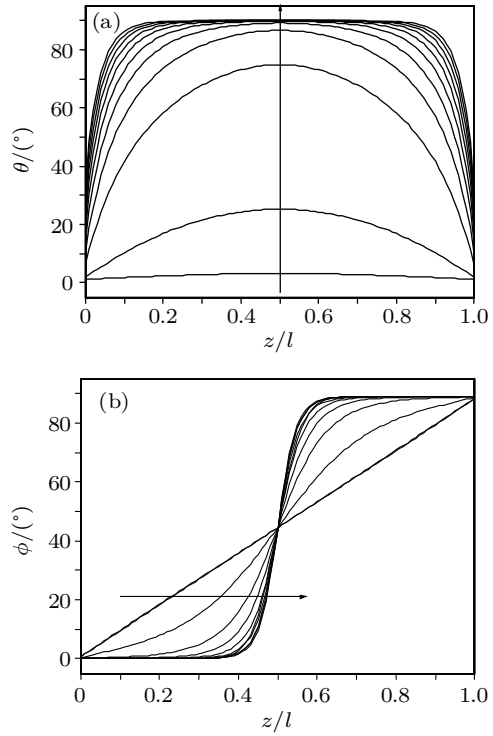


Fig. 4. Director distribution under the anchoring energy coefficient of 10^{-4} J/m^2 for different applied voltages; the applied voltage increases from 0 V to 10 V with a voltage step of 1 V along the arrow direction: (a) tilt angle and (b) twist angle.

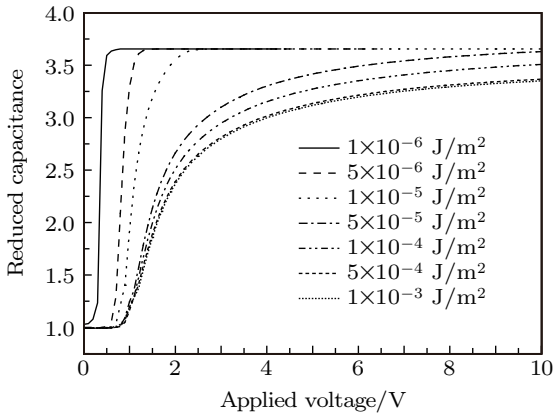


Fig. 5. Reduced capacitance of TN cell versus voltage for different anchoring energy coefficients.

As indicated in Fig. 6, the TN cell capacitance remains constant with increasing anchoring energy coefficient regardless of the applied voltage (2, 3, or 4 V). When the substrate anchoring energy coefficient exceeds 5×10^{-4} J/m^2, the difference in TN cell capacitance is small. For the same anchoring energy coefficient, the increase in the effective dielectric constant in the TN cell induced by the large tilt angle of the LC director on the substrate surface due to the enhanced applied voltage leads to the increase in the TN cell capacitance.

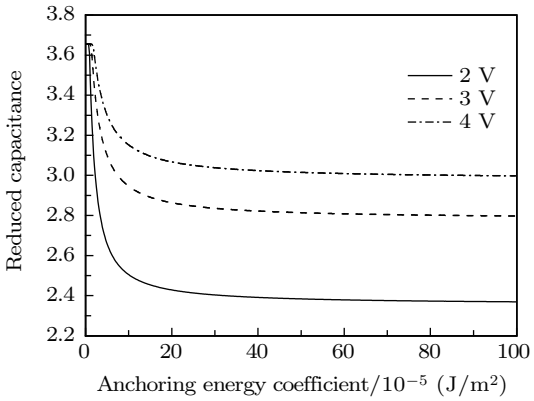


Fig. 6. Reduced capacitance of TN cell versus anchoring energy coefficient for different voltages.

3. Experimental design

3.1. Liquid crystal cell preparation

A TN cell is prepared in accordance with the following procedure: ITO glass cleaning→drying→orientation coating→curing→rubbing→cleaning→drying→silk-screen printing→sealant patterning→cell making→LC injecting→sealing. To vary the anchoring strength of the TN cell, three types of friction moment are utilized during substrate rubbing. The contact depth and rolling speed between the roller and the substrate varies. To obtain the TN cell, the rolling direction of the upper and lower substrates is perpendicular from 45° and 135°, respectively. The injecting LC E7 is acquired from Shijiazhuang Chengzhi Yonghua Display Materials Co., Ltd. Importantly, the whole process is conducted in a clean room.

3.2. Measurement of TN cell capacitance based on AC bridge

First, the circuit is connected, as shown Fig. 1, where the signal source provides the voltage of the AC bridge. Then, adjusting the precision resistance R and the fixed value capacitor C_2 makes the galvanometer show zero and the phase of points B and D be the same. The capacitance C_x of the TN cell can be achieved according to Eq. (2). Concurrently, the voltage between the upper and lower substrates can be tested. Similarly, groups of the voltage between the upper and lower substrates and the capacitance of the TN cell are obtained. Finally, the *C–U* experimental curve of the TN cell can be drawn using Origin software. The detailed process is as follows:

(i) In the experiment, the galvanometer is substituted with a digital multimeter (VC189, Victor), which is set to AC millivolt grade. The fixed value capacitor needed in the experiment is used. Resistances R_3 and R_4 are adjusted to the same proper

value. The testing voltage of the AC source varies from 0 V to 10 V, with the frequency 1 kHz.

(ii) The switch is turned on, the multimeter is connected between points B and D, and the potential difference is observed. These two balance conditions of amplitude and phase are supposed to be met. If the potential difference is not zero, then the AC bridge should be adjusted until the bridge is balanced by changing the values of R_2 and R_3.

(iii) When the multimeter reading is or almost zero, the voltage should be measured through a voltmeter (keeping two significant figures), and the capacitance of the TN cell can be achieved according to Eq. (2) based on the fixed value capacitance C_2.

(iv) The circuit is cut off, the value of C_2 is changed, and Steps (ii) and (iii) are repeated.

(v) With the voltage of the TN cell measured above as the horizontal coordinate and the ratio of TN cell capacitance and C_0 (the capacitance inferior to the threshold voltage) as the vertical coordinate, the C–U curve of the reduced capacitance of the TN cell versus voltage can be plotted.

To eliminate the influence of temperature on the TN cell capacitance, the precision hot stage (LTS350, Linkam) can be applied in the experiment to control the TN cell temperature to be 25 °C stable.

3.3. Comparison between experiment and theory

The experiment and theory can be compared by fitting of theoretical and experimental results. First, the C–U experimental curve based on the AC bridge is considered as the benchmark, and then the C–U theoretical curve for different anchoring energies is calculated. When both fully intend to fit, the anchoring energy used in the calculation is that on the substrate surface. Before fitting, the material parameters of the LC, including elastic and dielectric constants, and the device parameters of the TN cell, including cell gap and effective area of the substrate electrode, must be accurate and should be measured or offered by manufactures directly.

4. Discussion and conclusion

The LC cell can be regarded as a capacitor, in which the LC is a dielectric medium. The change in LC molecular orientation changes the effective dielectric constant of the LC cell, thereby affecting the LC cell capacitance. Therefore, factors that change the LC director all reflect the change in the LC cell capacitance, including the anchoring energy on the substrate surface. Ye *et al.*[24] designed the capacitance method to measure the flexelectric coefficient of the nematic LC because the flexelectric effect affects on the LC director.

In this study, we designed a method to measure the anchoring energy on the substrate surface using the AC bridge. The AC bridge is mainly composed of precision adjustable resistance, precision fixed value capacitor, and TN cell. By balancing the AC bridge, we can obtain the voltage and capacitance of the TN cell and the C–V experimental curve. Then, the anchoring energy on the substrate surface can be obtained by comparing with the numerical simulation C–V curve on the basis of Frank theory. Compared with other methods, this measurement does not need a complex optical path system, a high-precision instrument, and a harsh environmental condition. With only select precision adjustable resistance and precision fixed capacitor, the AC bridge can be assembled reasonably. Moreover measuring with high accuracy is easy, and the method can be applied to measure other performance parameters of LC devices, thereby expanding the means to measure the performance parameters of LC devices.

References

[1] Blinov L M and Chigrinov V G 1994 *Electrooptic Effects in Liquid Crystals Materials* (Berlin: Springer-Verlag) pp. 133–135
[2] Yang D K and Wu S T 2006 *Fundamentals of Liquid Crystal Devices* (New York: John Wiley & Sons Ltd) pp. 33–34
[3] Pasechnik S V, Chigrinov V G, Shmeliova D V, Tsvetkov V A, Kremenetsky V N, Liu Z J and Dubtsov A V 2006 *Liq. Cryst.* **33** 175
[4] Sun Y B, Ma H M and Zhang Z D 2002 *Liq. Cryst.* **29** 1059
[5] Jo S I, Choi S W, Lee Y J, Moon Y K, Yang Y C, Yu C J and Kim J H 2011 *J. Appl. Phys.* **109** 084501
[6] Takemi T, Oka S, Kimura M and Akahane T 2004 *Jpn. J. Appl. Phys.* **43** 7629
[7] Liou W R, Chen C Y, Ho J J, Hsua C K, Changa C C, Hsiaoc R Y and Changa S H 2006 *Displays* **27** 69
[8] Karmin C K and Livesey K L 2014 *Liq. Cryst.* **41** 707
[9] Ye W J, Xing H Y, Zhou X, Sun Y and Zhang Z 2015 *AIP Adv.* **5** 067145
[10] Hamaguchi S, Otsuka Y, Taga Y, Motohiro T and Itoh T (U.S. Patent) 4 813 768 [1989-03-021]
[11] Shan J, Shi W, Liu L Y, Shen Y R and Xu L 2012 *Phys. Rev. Lett.* **109** 147801
[12] Rosenblatt C 1984 *J. Phys.* (Paris) **45** 1087
[13] Yang K H and Rosenblatt C 1983 *Appl. Phys. Lett.* **43** 62
[14] Yang F, Ruan L and Sambles J R 2000 *J. Appl. Phys.* **88** 6175
[15] Yokoyama H and Van Sprang H A 1985 *J. Appl. Phys.* **57** 4520
[16] Nastishin Y A, Polak R D, Shiyanovskii S V and Lavrentovich O D 1999 *Appl. Phys. Lett.* **86** 4119
[17] Toko Y and Akahane T 2001 *Mol. Cryst. Liq. Cryst.* **368** 469
[18] Murauski A, Chigrinov V. Muravsky A, Yeung, F S, Ho J and Kwok H S 2005 *Phys. Rev. E* **71** 061707
[19] Ye W J, Liu X S, Song X L and Zheng G L 2014 *Chin. J. Liq. Cryst. Disp.* **29** 686
[20] Sugimura A, Luckhurst G R and Ou-yang Z C 1995 *Phys. Rev. E* **52** 681
[21] Wang Q and He S L 2011 *Acta Phys. Sin.* **50** 926 (in Chinese)
[22] Chen H W, Zhu R D, Zhu J X and Wu S T 2015 *Liq. Cryst.* **42** 1738
[23] Stephen William Morris 1985 "Measurements of the Elastic Constants of a Liquid Crystal", MS Thesis (Vancouver: University of British Columbia)
[24] Ye W J, Xing H Y, Cui W J, Zhou X, Sun Y and Zhang Z D 2014 *Chin. Phys. B* **23** 116101